Observation of a 2D Bose Gas: From Thermal to Quasicondensate to Superfluid

P. Cladé,* C. Ryu,† A. Ramanathan, K. Helmerson, and W. D. Phillips

Atomic Physics Division, National Institute of Standards and Technology, Gaithersburg, Maryland 20899-8424, USA and Joint Quantum Institute, NIST and University of Maryland, College Park, Maryland 20742, USA

(Received 20 May 2008; published 27 April 2009)

We present experimental results on a Bose gas in a quasi-2D geometry near the Berezinskii, Kosterlitz, and Thouless (BKT) transition temperature. By measuring the density profile after time of flight and the coherence length, we identify different states of the gas. We observe that the gas develops a bimodal distribution without long range order. In this regime, the gas presents a longer coherence length than the thermal cloud; it is quasicondensed but is not superfluid. Experimental evidence indicates that we also observe the superfluid transition (BKT transition). For a sufficiently long time of flight, we observe a trimodal distribution when the gas has developed a superfluid component.

DOI: 10.1103/PhysRevLett.102.170401 PACS numbers: 03.75.Lm, 67.25.dj, 67.85.−d

One of the most fascinating aspects of a Bose gas in the degenerate regime is the role of dimensionality. A two-dimensional (2D) interacting Bose gas is superfluid [1,2] at a temperature T below the Berezinskii-Kosterlitz-Thouless (BKT) transition temperature T_{BKT}. However, in contrast to the three-dimensional (3D) case, there is no long range coherence (no condensate) and the coherence decays as a power law [1,2]. At T above T_{BKT}, proliferation of free vortices suppresses superfluidity. The decay of coherence changes from algebraic to exponential with a characteristic length ξ, which diverges at T_{BKT} and remains significantly larger than the thermal de Broglie wavelength ($\lambda = \sqrt{2\pi\hbar^2/Mk_BT}$, where M is the atomic mass) over a range of $T > T_{\mathrm{BKT}}$. Furthermore, near the transition only phase fluctuations are significant and density fluctuations are suppressed. Following [3], we refer to this region as the ''nonsuperfluid quasicondensate,'' which has approximately uniform phase in regions of size ξ. As T is increased further, ξ gradually reduces and approaches λ, density fluctuations gradually increase, and the gas crosses over from the nonsuperfluid quasicondensate to a thermal Bose gas.

Experiments on 2D bosonic systems, such as ^{4}He films [4] and trapped Bose gases [5,6] show signatures of the BKT transition. Other systems, such as arrays of Josephson junctions [7] and a 2D lattice of (3D) Bose-Einstein condensates [8], also exhibit a similar transition. Intriguingly, a reduction in three-body dipolar recombination (which is usually associated with condensation) was observed well above T_{BKT} in 2D spin polarized atomic hydrogen on liquid ^{4}He [9]. This observation results from a reduction of density fluctuations, i.e., quasicondensation [3]. While these experiments generally support the BKT theory, which was formulated for a homogeneous system, a complete understanding of finite systems still remains a challenge, especially when the systems are not close to the thermodynamic limit [10]. These finite 2D systems open up new questions on the relationship between superfluidity and Bose-Einstein condensation (BEC), where the contrast between the two phenomena may be more pronounced. Theoretical treatments of such atomic-gas systems [5,6] have used classical-quantum field [11], quantum Monte Carlo [12], and mean-field Hartree-Fock methods [13,14].

We present evidence, from experiments in a weakly interacting, quasi-2D Bose gas, of a crossover from thermal (normal) to quasicondensate (QC) without superfluidity and then a sharp (BKT) transition to superfluid QC. We explicitly identify the theoretically expected nonsuperfluid QC, a feature not seen in other experiments on a more strongly interacting, 2D trapped, Bose gas [5,6]. We use an interferometric method to study the coherence of the gas down to distances smaller than λ.

The BKT transition occurs at a universal value of the superfluid density $n_s = 4/\lambda^2$. However, the total density at the transition, n_{BKT}, is not universal and depends on the strength of the interactions [1]. Interactions in a weakly interacting Bose gas trapped in a quasi-2D geometry (tight confinement with large frequency ω_0 along one axis) are described by a dimensionless coupling constant $\tilde{g} = a\sqrt{8\pi M\omega_0/\hbar}$ [15], where a is the 3D scattering length. In the limit of weak interactions, $n_{\mathrm{BKT}}\lambda^2 = \ln(C/\tilde{g})$ [16,17]. Monte Carlo simulations that calculate the density as a function of the chemical potential give $C \approx 380$ [18]. We use those simulations for our trapped system by applying a local density approximation (LDA) (see Ref. [18]). This is valid near T_{BKT} if the healing length at T_{BKT}, $r_c \simeq 2\lambda/\sqrt{2\pi\tilde{g}}$ is smaller than the typical size R of the region where interactions play a significant role (from the chemical potential in [18], we find that $R \approx \sqrt{\tilde{g}}R_T$, where $R_T = \sqrt{2k_BT/m\omega_\perp^2}$ is the size of the thermal cloud, $\omega_\perp$ being the frequency of the trap in the 2D plane). Hence to satisfy the LDA and thus have a BKT transition at a temperature higher than the true BEC transition [19], one must satisfy $\hbar\omega_\perp < \tilde{g}k_BT$. For our typical parameters, $\tilde{g} \simeq 0.02$, $T \simeq 100$ nK and $\omega_\perp/2\pi \simeq 20$ Hz, so LDA is reasonable.

In the thermodynamic limit, a trapped noninteracting 2D gas can Bose-condense [20]. Taking into account the interactions in the trapped system by applying the LDA to the calculation of Refs. [18], we get for fixed λ (Fig. 1) the total central density versus the total number of atoms N (normalized to the BEC critical number for 2D trapped, noninteracting atoms, $N_{\rm crit} = \pi^2/6[k_BT/\hbar\omega_\perp]^2$ [20]). When N approaches $N_{\rm crit}$, the central density increases rapidly and a bimodal distribution appears (Fig. 1, inset). This coincides with a reduction in density fluctuations, which Refs. [18] associate with the appearance of a quasicondensate. The BKT transition occurs at $N/N_{\rm crit} \approx 1.05$, where the central density is $n_{\rm BKT}$. We do not expect to see a dramatic change of the *in situ* spatial density profile at the BKT phase transition, because it affects mainly the phase coherence. Phase coherence is revealed in our experiments by time of flight (TOF) expansion or by interferometry. By all these methods, we see the progression from thermal to quasicondensate to superfluid.

Our experiment uses sodium atoms confined in a single, horizontal, quasi-2D, optical dipole trap, similar to that described in [21]. An infrared (1030 nm) trap laser beam is spatially filtered, focused into a sheet of light using a cylindrical lens and projected onto the atomic cloud using a telescope. The sheet has a waist ($1/e^2$ radius) in the vertical direction of ≈ 9 μm, and a Rayleigh range of 440 μm. The other waist is 800 μm; however, atoms see a stronger confinement due to a small distortion of the laser intensity profile in this direction. This results in a trapped cloud of atoms that is approximately a circular disk with an aspect ratio of 50. For a typical value of the laser power (500 mW), the trapping frequencies are 1 kHz and 18 Hz in the vertical and horizontal directions, respectively.

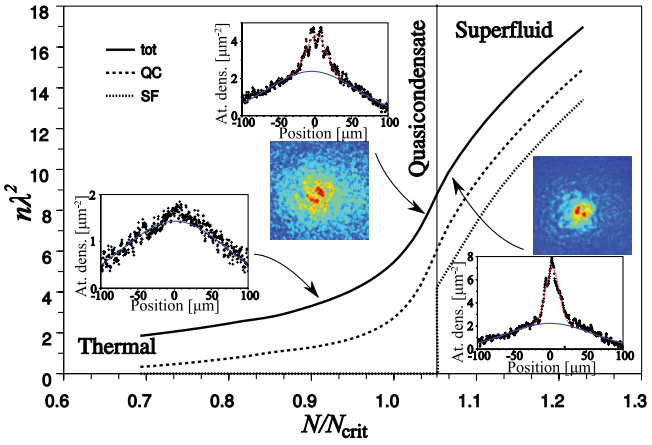

FIG. 1 (color). Calculated total density (tot), quasicondensate (QC) density, and superfluid (SF) density at the center of the cloud in a 2D trap versus the total number of atoms N normalized to $N_{\rm crit}$, the critical number for BEC of a 2D trapped, noninteracting gas. Insets: representative images and corresponding density profiles, measured along a line passing through the center of the cloud, for different N after 5 ms TOF. The dot-dashed (red) line is a fit to the sum of two Gaussians, while the solid (blue) line is the wider Gaussian.

We initially confine the atoms in a magnetic trap and cool them using rf-induced evaporation [22]. Before reaching BEC, we adiabatically transfer the atoms to the optical dipole trap. After 5 s of evaporation in the dipole trap, we reduce the depth (initially around 5 μK) during 1 s to a final value ranging from 5 to 2 μK and then hold for 5 s to complete the evaporative cooling. We set the final temperature by choosing the final trap depth. We vary the phase space density keeping T constant (same trap depth) by varying the initial number of trapped atoms by about a factor of 10. This results in a 20% variation in the final number of atoms. For a trap with a vertical confinement of $\omega_0/2\pi = 1$ kHz, T is around 100 nK, which corresponds to $k_BT \approx 2\hbar\omega_0$, so the thermal motion is not completely frozen out along the tight direction. However, the quasicondensed atoms are well confined in 2D since the mean field never exceeds 1 kHz, and therefore we expect to see 2D physics.

We perform absorption imaging along the vertical direction, after turning off the trap and waiting for a TOF period, to obtain the 2D density profile of the released atomic cloud. The insets of Fig. 1 show two such absorption images after 5 ms of TOF, for the same temperature but a different number of atoms. Both pictures show bimodality [23] and large density fluctuations. These fluctuations, which appear only after TOF, are due to the *in situ* phase fluctuations of the quasicondensate. This is in contrast to the situation for a true (3D) Bose-Einstein condensate, which also has a bimodal spatial density distribution in TOF, but is much smoother.

In Fig. 2 we plot the width of the narrow part of the bimodal distribution (Fig. 1, insets) as a function of the peak total density for two different T (trap depths). For both T, the width initially decreases with increasing density (presumably due to an increase in coherence) and then, beyond a certain point, increases slowly (presumably due to repulsive interactions between atoms). Calculations show that the width of the narrow peak in the *in situ* density distribution exhibits a minimum at the appearance of superfluidity in the trapped 2D Bose gas [24]. This suggests identifying our minimum with the BKT transition. In the inset we plot the density [25] at the minimum width as a function of T. The dashed line is the theoretical prediction $n_{\rm BKT}\lambda^2 = \ln(380/\tilde{g})$ [18] and the continuous line is this prediction corrected by a factor taking into account thermal excitation of modes in the tight direction, as done in Ref. [13]. The position of the point of minimum width agrees with the corrected theoretical prediction, supporting its identification as the BKT transition in the center of the trap.

With this interpretation, the central inset profile in Fig. 1 is for $T > T_{\rm BKT}$ and contains a broad thermal component and a narrow nonsuperfluid quasicondensate. The right-hand inset for $T < T_{\rm BKT}$ is also bimodal and presumably the QC portion contains both a superfluid and nonsuperfluid component, which are not separated after 5 ms TOF. After 10 ms of TOF, however, the three components can be separated. For T just above $T_{\rm BKT}$, there is a bimodal

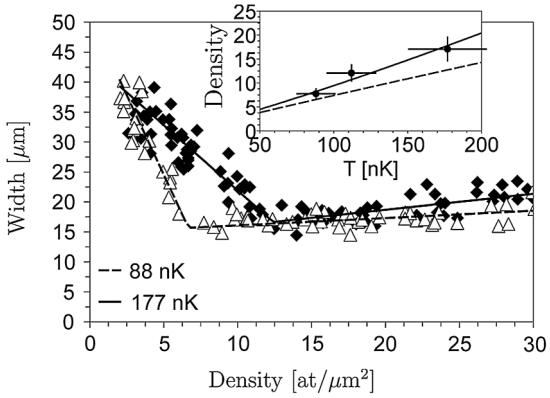

FIG. 2. Width of the narrow part of the cloud from fits of 5 ms TOF images by two Gaussians (see insets of Fig. 1) versus the fitted peak 2D density, for two different temperatures. The intersection of linear fits to two portions of the data is used to determine a transition point. Inset: 2D "*in situ*" peak density [25] at the transition point as a function of the temperature. The dashed line is the theoretical value $n_{\mathrm{BKT}}\lambda^2 = \ln(380/\tilde{g})$ and the solid line is the same value corrected using a 3D model [13]. We add a $\pm 15\%$ uncertainty [27] primarily due to the disagreement of the different methods used for calibration of the temperature and density.

distribution (Fig. 3, left): the thermal component [solid (blue)] and quasicondensate [dot-dashed (red)]. For T just below T_{BKT} (Fig. 3, right), we see a trimodal distribution: the thermal component and the nonsuperfluid QC (which are very similar to the case of T just above T_{BKT}) and the superfluid part [very narrow peak, dashed (orange)]. This transition occurs when the central density exceeds ≈ 4.5 atoms/μm^2. With the approximate correction factor [25], the *in situ* density is ≈ 9.4 atoms/μm^2, in good agreement with the theoretical prediction and the 5 ms TOF analysis.

To measure the coherence of the gas on a length scale below λ, we developed a Ramsey-like method that uses two $\pi/2$, 2-photon Raman pulses between the $F = 1$ and $F = 2$ ground hyperfine states, but with counterpropagating and nearly counterpropagating laser beams that transfer two units of photon momentum to the atoms. We observe the *in situ* interference of two copies of the cloud, which have a velocity difference of $\hbar\mathbf{K}/m$, where $\mathbf{K} = \mathbf{k_1} - \mathbf{k_2} - \mathbf{k_1'} + \mathbf{k_2'}$ (notation defined in Fig. 4) and a spatial separation of $\mathbf{R} = \hbar(\mathbf{k_1} - \mathbf{k_2})\tau/m$ from the displacement of the cloud during the time τ between pulses, by imaging atoms in only one ($F = 2$) hyperfine state. Specifically, if $\hat{\psi}_0(\mathbf{r})$ is the quantum field operator, with $n_0(\mathbf{r}) = \langle \hat{\psi}_0^\dagger(\mathbf{r})\hat{\psi}_0(\mathbf{r})\rangle$ the initial atomic density (in $F = 1$), then the measured density of atoms in $F = 2$ after the two Raman pulses is

$$\tfrac{1}{4}[2n_0(\mathbf{r}) + \langle \hat{\psi}_0^\dagger(\mathbf{r})\hat{\psi}_0(\mathbf{r} - \mathbf{R})e^{i\mathbf{r}\cdot\mathbf{K}+i\phi_0} + \mathrm{H.c.}\rangle], \quad (1)$$

where ϕ_0 is the (uncontrolled) phase between the two Raman pulses. By measuring the average spatial contrast of the interference fringes in an image, for several images of varying $\mathbf{R}$, we can extract the normalized correlation function $g^{(1)}(\mathbf{R}) = \langle \hat{\psi}_0^\dagger(\mathbf{r})\hat{\psi}_0(\mathbf{r} - \mathbf{R})\rangle/n_0(\mathbf{r})$.

Figure 5 shows the average contrast of the central five fringes as a function of $\mathbf{R}$, for different densities at $T \approx 100$ nK. This contrast is determined by measuring the amplitude of the Fourier component of the image at the spatial frequency of the fringes, relative to the peak density of the fringes. Since we cannot precisely control the number of atoms, we average only the measured contrast that falls within a chosen range of peak densities. For each curve we see an initial drop of the contrast on a length scale of order 1 μm, due to the relatively short coherence length of the thermal component ($\lambda \cong 1$ μm for $T = 100$ nK). For densities between 5 and 8 atoms/μm^2 (dotted line), where we clearly see a bimodal distribution, the coherence extends well beyond λ, but decreases to zero by 10 μm, a distance much shorter than the spatial width of the narrow part of the bimodal distribution (see inset). This behavior is as expected for this QC region of T just above T_{BKT} where, due to local condensation, there is coherence for distances greater than λ, but the coherence decreases exponentially on a length scale of the order of the healing length, $r_c \simeq 6$ μm [18]. For higher densities ($T < T_{\mathrm{BKT}}$), the coherence also decays slowly but has a nonzero value even at 20 μm. Here, one expects a power law decay of the coherence mainly due to long wavelength phonons [15].

In this experiment, we have observed the predicted intermediate regime between the thermal and the superfluid phase, characterized by a bimodal density distribution and a coherence length longer than λ, but smaller than the width of the peak of the bimodal distribution. At higher densities, significant coherence persists over much longer

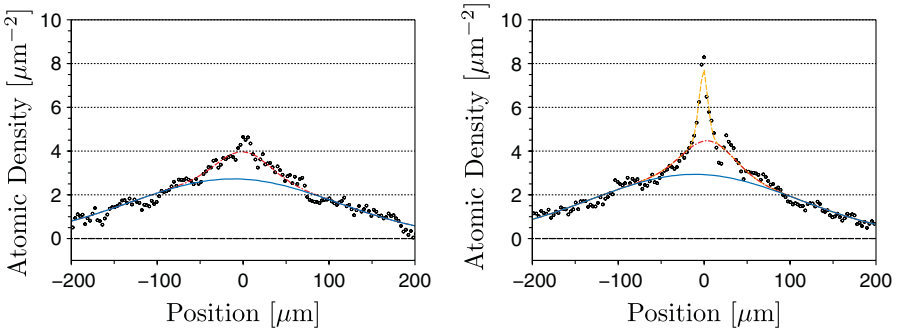

FIG. 3 (color). Cross section of the density profile of the cloud after 10 ms of TOF, fitted with the sum of three Gaussians for $T \approx 100$ nK. Left: for $n < n_{\mathrm{BKT}}$ ($T > T_{\mathrm{BKT}}$); right: for $n > n_{\mathrm{BKT}}$ ($T < T_{\mathrm{BKT}}$).

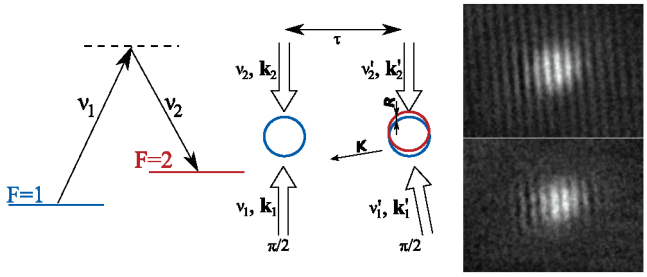

FIG. 4 (color). Left: Schematic of the atom interferometer used to measure the spatial coherence of the 2D atomic cloud. The Raman laser beams have frequencies ν_i and corresponding wave vectors $\mathbf{k}_i$. Right: Images of atoms in the $F = 2$ state after the interferometer sequence for two different delays between Raman pulses (upper: $\tau = 7.5$ μs, lower: $\tau = 17.5$ μs). For the longer delay, the interference of the thermal cloud is washed out and there are only fringes from the superfluid region, which has a longer coherence length.

distances, which is consistent with the BKT superfluid phase. For sufficiently long TOF we clearly see a trimodal distribution showing the presence of three components. In previous experiments [5,6] the intermediate nonsuperfluid QC was not distinguished from the thermal cloud. This may be because our $\tilde{g}$ is 6 or 7 times smaller than in the experiments of [5,6]. Also, their imaging integrates over one dimension of the 2D geometry, reducing the narrow part of the distribution relative to the thermal cloud. However, recent experiments by this group, using a geometry similar to ours that allows imaging of the 2D spatial profile of the gas, still does not exhibit a trimodal distribution [26]. Finally, while our results seem consistent with a 2D description, our thermal gas is not strictly confined in 2D. Further studies would elucidate whether these differences account for the observation of the nonsuperfluid QC and trimodal behavior seen in our experiment, but not in the experiments of [5,6].

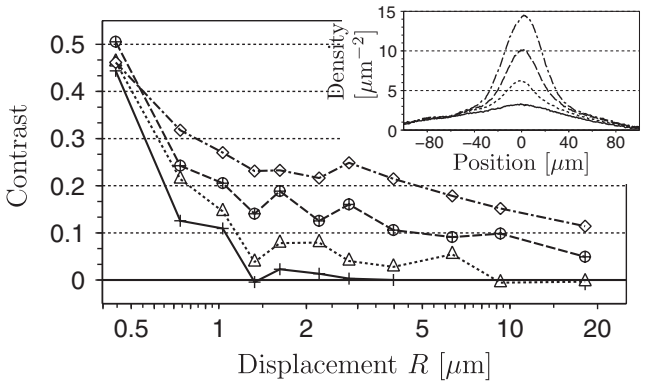

FIG. 5. Contrast of the interference fringes as a function of the separation of the two clouds in the interferometer. Each curve corresponds to an average over many data sets where the maximum density of atoms falls within a chosen range. Inset: Corresponding density profiles of the atomic cloud. Lines (solid, dotted, dashed, dot-dashed) correspond, respectively, to density ranges of 2–4, 5–8, 10–12, 13–19 atoms/μm^2.

Our experimental setup, which allows us to see BKT related physics in a single "pancake" of atoms, opens new opportunities, such as studying density fluctuations at the transition. Future experiments could also explore different interaction regimes by using a Feshbach resonance to tune the coupling constant, as well as study the behavior of the superfluid transition, going from a 3D to a purely 2D Bose gas.

This work was supported by the Office of Naval Research. We thank J. Dalibard, Z. Hadzibabic, P. Krüger, T. Simula, M. Davis, and B. Blakie for helpful discussions.

*Permanent Address: Laboratoire Kastler Brossel, UPMC, CNRS, ENS, Paris, France.
†Present Address: Quantum Institute, LANL, Los Alamos, NM, USA.

[1] J. M. Kosterlitz and D. J. Thouless, J. Phys. C **6**, 1181 (1973).
[2] V. L. Berenzinskii, Sov. Phys. JETP **34**, 610 (1972).
[3] Y. Kagan *et al.*, Phys. Rev. A **61**, 043608 (2000).
[4] D. J. Bishop and J. D. Reppy, Phys. Rev. Lett. **40**, 1727 (1978).
[5] Z. Hadzibabic *et al.*, Nature (London) **441**, 1118 (2006).
[6] P. Krüger *et al.*, Phys. Rev. Lett. **99**, 040402 (2007).
[7] D. J. Resnick *et al.*, Phys. Rev. Lett. **47**, 1542 (1981).
[8] V. Schweikhard, S. Tung, and E. A. Cornell, Phys. Rev. Lett. **99**, 030401 (2007).
[9] A. I. Safonov *et al.*, Phys. Rev. Lett. **81**, 4545 (1998).
[10] S. T. Bramwell and P. C. W. Holdsworth, Phys. Rev. B **49**, 8811 (1994).
[11] R. N. Bisset *et al.*, Phys. Rev. A **79**, 033626 (2009).
[12] M. Holzmann and W. Krauth, Phys. Rev. Lett. **100**, 190402 (2008).
[13] M. Holzmann *et al.*, Europhys. Lett. **82**, 30001 (2008).
[14] Z. Hadzibabic *et al.*, New J. Phys. **10**, 045006 (2008).
[15] D. Petrov *et al.*, J. Phys. IV (France) **116**, 5 (2004).
[16] V. Popov, *Functional Integrals in Quantum Field Theory and Statistical Physics* (Reidel, Dordrecht, 1983).
[17] D. S. Fisher and P. C. Hohenberg, Phys. Rev. B **37**, 4936 (1988).
[18] N. Prokof'ev *et al.*, Phys. Rev. Lett. **87**, 270402 (2001); Phys. Rev. A **66**, 043608 (2002).
[19] D. Petrov *et al.*, Phys. Rev. Lett. **84**, 2551 (2000).
[20] V. Bagnato and D. Kleppner, Phys. Rev. A **44**, 7439 (1991).
[21] A. Görlitz *et al.*, Phys. Rev. Lett. **87**, 130402 (2001).
[22] M. Kozuma *et al.*, Phys. Rev. Lett. **82**, 871 (1999).
[23] We use the term bimodality to describe the two peak character of the density distributions without implying a two fluid or component picture as in the case of a 3D BEC.
[24] M. J. Davis and P. B. Blakie (unpublished).
[25] In order to account for expansion in TOF, we multiply by $1 + \omega_\perp^2 t_{\mathrm{TOF}}^2$ to bring the density back to its *in situ* value. This correction factor is true only for the thermal part and probably overestimates the *in situ* density of the QC part.
[26] J. Dalibard (private communication).
[27] Unless otherwise stated, the uncertainties are 1 standard deviation combined systematic and statistical.